Computers, Materials & Continua

Tech Science Press

https://doi.org/10.32604/cmc.2026.078029

ARTICLE

KBGWO-RNP: Knowledge-Based Grey Wolf Optimizer for Multi-Criteria RFID Network Planning in Medical Asset Monitoring

Mohamad Khairi Ishak[1], **Samir Ait Lhadj Lamin**[2,3], **Mohammad Shokouhifar**[4,*], **Aseel Smerat**[5], **Kamal M. Othman**[6], **Abdulfattah Noorwali**[6] **and Esam Y.O. Zafar**[6]

[1]Department of Computer Engineering, College of Computing and Informatics, University of Sharjah, Sharjah, United Arab Emirates
[2]Graduate School of Health Sciences Engineering, Mohammed VI University of Sciences and Health, Casablanca, Morocco
[3]Laboratory of Mathematics, Statistics and Applications, Faculty of Sciences, Mohammed V University in Rabat, Rabat, Morocco
[4]Institute of Research and Development, Duy Tan University, Da Nang, Vietnam
[5]Hourani Center for Applied Scientific Research, Al-Ahliyya Amman University, Amman, Jordan
[6]Department of Electrical Engineering, College of Engineering & Architecture, Umm Al-Qura University, Makkah, Saudi Arabia

*Corresponding Author: Mohammad Shokouhifar. Email: mohammadshokouhifar@duytan.edu.vn

Received: 22 December 2025; Accepted: 25 May 2026; Published: 23 July 2026

ABSTRACT: Radio Frequency Identification (RFID) has emerged as an effective remote technology for real-time monitoring and management of medical assets in hospitals. Most existing RFID Network Planning (RNP) methods are primarily based on either heuristic or metaheuristic approaches. While heuristic approaches are computationally efficient and converge rapidly, they often suffer from premature convergence and suboptimal network configurations. Conversely, metaheuristic algorithms provide stronger global search capabilities and improved solution quality, but they typically require higher computational effort and may still exhibit stagnation in local optima when applied to complex hospital layouts. To overcome these limitations while utilizing the strengths of both paradigms, this paper proposes a Knowledge-Based Grey Wolf Optimizer for RNP, referred to as KBGWO-RNP. The proposed method integrates the global exploration capability of the metaheuristic-driven search with knowledge-based heuristic operators that guide local search and refinement. In particular, the framework incorporates domain-specific knowledge to enhance antenna placement decisions and improve convergence behavior. The KBGWO-RNP framework supports directional antennas with varying coverage profiles. A multi-criteria objective function is formulated to increase the network coverage while simultaneously reducing inter-antenna interference and deployment cost. Extensive simulation experiments conducted on a hospital layout demonstrate that the proposed KBGWO-RNP framework consistently outperforms conventional heuristic and metaheuristic baselines. The results show that the proposed method achieves a coverage rate of 90.4% while maintaining the interference level at 19.9%, indicating a strong balance between performance different objectives. Furthermore, ablation analysis confirms that the integration of knowledge-based guidance with metaheuristic search significantly improves both solution quality and stability. The proposed framework offers a balanced trade-off between computational efficiency and optimization performance, and demonstrating clear advantages over existing approaches.

KEYWORDS: RFID network planning (RNP); medical asset tracking; coverage; interference; heuristic information; grey wolf optimizer (GWO)

1 Introduction

Medical asset management is a critical challenge in hospital environments, as it is essential for ensuring timely access to equipment and reducing the risk of loss or theft. Hospitals manage numerous high-value movable assets, including surgical instruments, defibrillators, portable ventilators, pulse oximeters, wheelchairs, and beds, all of which are vulnerable to misplacement or unauthorized removal. In addition, hospital staff often spend considerable time searching for missing equipment, leading to operational inefficiencies. As a result, manual asset management methods are increasingly inadequate, highlighting the need for automated information systems to improve asset visibility and utilization [1].

Traditional asset monitoring solutions such as barcode systems are constrained by line-of-sight requirements and limited operational speed. In this case, Radio Frequency Identification (RFID) technology offers an effective automated solution for real-time tracking of both static and mobile assets through wireless communication within hospital environments. Unlike barcodes, RFID systems can identify objects without line-of-sight constraints and can detect a large number of tagged items simultaneously within a reader's coverage area [2]. Given the frequent movement and shared use of medical devices across departments, RFID offers a practical approach for continuous facility-wide monitoring, significantly reducing asset loss and improving operational efficiency [3].

Planning RFID networks planning (RNP) is recognized as an NP-hard challenge [4], and thus, the majority of prior research tackles it using either heuristics or metaheuristics [5]. Heuristics are appreciated for their straightforwardness and computational efficiency, making them well-suited for real-time applications or environments with limited resources [6]. However, they typically lack extensive global search capabilities and may face difficulties when handling complex RNP scenarios with multiple objectives. On the other hand, metaheuristic algorithms utilize nature-inspired strategies to explore the solution space more broadly, facilitating improved compromises among multiple RNP-based objective functions. Consequently, hybrid approaches that combine the strengths of both heuristics and metaheuristics are particularly promising for effective RNP solutions.

Despite their usefulness, existing RNP methods face several challenges that limit their effectiveness in hospitals. For example, models using omnidirectional antennas, while providing wide coverage in general applications, often suffer from excessive overlap and high interference, making them unsuitable for indoor hospital corridors. Additionally, many RNP models simplify the problem by considering only a single antenna type, reducing the task to basic node placement. From an algorithmic perspective, the majority of metaheuristics depend on random starting points and standard population update procedures, without utilizing knowledge from the network or environmental structure. These limitations often result in sub-optimal solutions that lack adaptability and efficiency, particularly in resource-constrained hospital settings.

To overcome the limitations of existing methods in both network modeling and solution strategies, we propose a hybrid solution that combines heuristic knowledge with metaheuristic search. In the proposed method, heuristic knowledge is utilized to evaluate candidate antenna configuration parameters (i.e., type, read range, beam width, and direction) based on structural factors including zone criticality, proximity to wall, and coverage/interference correlations with other deployed antennas. Incorporating this knowledge-based guidance directs the metaheuristic search more effectively, leading to higher-quality solutions and faster convergence. The proposed multi-criteria framework ensures balanced trade-offs among coverage, interference, and deployment cost. Specifically, the main contributions of this paper are:

- Introducing a Knowledge-Based Grey Wolf Optimizer for RNP (termed as KBGWO-RNP), as a hybrid computationally efficient optimization-level RNP framework under abstracted indoor propagation assumptions for asset monitoring in hospitals.

- Considering directional RFID antennas with heterogeneous attributes including read range, beamwidth, and cost, to enable generating coverage-effective and cost-efficient configuration with the minimum interference level.
- Developing a Knowledge-Based Heuristic (KBH) algorithm to generate importance scores of antenna placement, considering structural and environmental factors including zone criticality, wall proximity, corner distances, and correlation with already placed antennas.
- Utilizing a hybrid enhanced Grey Wolf Optimizer (GWO) equipped with KBH local search operators, adopting a multi-criteria fitness function to maximize total criticality-aware coverage, while reducing inter-antenna interference and deployment cost.
- Justifying the performance of the KBGWO-RNP model through testing in a hospital plan.

The structure of the paper is as follows: Section 2 provides a review of related work, Section 3 introduces the network model, and Section 4 details the KBGWO-RNP framework. Section 5 presents the experimental results and comparative analysis, while Section 6 concludes the study.

2 Literature Review

Typically, an RFID system consists of readers, antennas, tags, and a central host computer. Tags store object information via a microchip, antenna, and memory, each with a unique ID, and are available as passive, active, or semi-passive types in various sizes [7]. Readers collect and decode tag data using one or more antennas and communicate with nearby tags, while interfacing with host systems via standard protocols such as IEEE 802.11 or IEEE 802.3 [8]. The host computer manages this information in a back-end database and coordinates data exchange across enterprise systems [9]. Antennas vary in polarization, bandwidth, direction, read range, and beam width; directional antennas offer focused coverage and reduced interference, making them suitable for RNP in complex hospital environments, whereas omnidirectional antennas provide broader coverage but are more prone to interference in dense deployments [10].

Recent advances in RFID system design have increasingly focused on improving tag-level performance through flexible materials and energy harvesting technologies, which directly enhance deployment feasibility in healthcare environments. Flexible and wearable RFID antennas have been proposed to support integration into biomedical and environmental sensing platforms, while maintaining stable RF performance under mechanical deformation. For instance, flexible transparent antenna systems combined with RF and solar energy harvesting have demonstrated efficient hybrid power generation, enabling autonomous operation of wearable devices and distributed sensors. Similarly, hybrid RF-solar harvesting architectures integrated with RFID tags have been shown to extend tag functionality and improve read range by efficiently managing harvested energy through rectifier circuits and power management modules [11]. Beyond solar-based solutions, semi-passive UHF RFID sensor tags incorporating energy harvesting modules or battery-assisted designs have been widely investigated to extend communication range and support energy-demanding sensing operations, highlighting the importance of energy-aware tag design and communication link optimization [12]. Furthermore, recent developments in textile-based and flexible RFID tags integrating solar and thermal energy harvesting mechanisms have demonstrated significant improvements in read range, in some cases achieving up to two-fold enhancement compared to conventional passive tags, thereby reinforcing their suitability for wearable and smart hospital applications [13]. These advancements indicate a clear trend toward multifunctional RFID tags that combine mechanical flexibility, energy autonomy, and improved RF performance, which are essential for next-generation healthcare monitoring systems.

Given the NP-hard nature of RNP, most solution methods rely on heuristics or metaheuristics, which are discussed in the following.

2.1 Heuristic Approaches

Over the past years, various heuristic-based RNP approaches have been developed to address different challenges. For example, Gupta and Iyer [14] proposed two heuristic-based RNP models to incorporate driver design, antenna range calculations, and a reader emulator for coverage optimization in obstacle-free environments. Mysore et al. [15] utilized a geometry-driven Graham scan to achieve complete coverage with the minimum number of readers. Liu et al. [16] introduced a federated framework to coordinate readers, mitigating reader-tag and reader-reader collisions. Qu et al. [17] integrated RFID with Markov chain models to improve equipment access and management within supply chains, and Tsai et al. [18] proposed a real-time tracking system for mobile healthcare assets. Moreover, Nhat [19] presented a Hopfield Network for RNP Optimization (HNRNPO) specifically for space-constrained clinical settings.

2.2 Metaheuristic Approaches

Metaheuristic approaches have been widely used to address different RNP challenges [20]. For instance, Dimitriou et al. [21] utilized Particle Swarm Optimization (PSO) to improve network coverage, limit interference, and cut overall costs. Shi et al. [22] utilized Chicken Swarm Optimization (CSO) to determine optimal antenna placement, while Cuckoo Search (CS) was applied to distribute reader loads efficiently and reduce energy consumption [23]. An evolutionary-based Genetic Algorithm (GA) has also been applied to optimize networks with both directional and omnidirectional antennas [24], and a hybrid GA-PSO model was developed for planning readers to track predictable mobile tags [25]. Xu et al. [26] integrated Monte-Carlo simulations into PSO to improve robustness under uncertainty, while Yuan et al. [27] presented a multi-objective Bacterial Foraging Optimization (BFO) combining adaptive search strategies, multi-cell communication, and indicator-based preference metrics.

Recent studies have further advanced RNPs. Shokouhifar [28] developed a hybrid RNP solution method using Simulated Annealing (SA) and Whale Optimization Algorithm (WOA). Mohammed et al. [29] combined Birch clustering with Chaotic PSO to achieve a balance between coverage and interference. Knapp and Romagnoli [30] applied GAs to reduce the number of antennas without compromising accuracy, while Zheng et al. [31] utilized multiple local search operators to improve convergence. Abdulbaqi and Abdullah AL-Khalidi [32] tackled RNP from a topological perspective using PSO, and Maimouni et al. [33] developed a neural-inspired metaheuristic, named IRAENNA, to optimize antenna deployment.

2.3 Hybrid Approaches

There are also some hybrid metaheuristic-based approaches. For instance, Ma et al. [34] integrated a fuzzy model to select appropriate solutions from Pareto Fronts in a multi-criteria RNP. Lu and Yu [35] formulated RNP as a constrained optimization problem using a fuzzy k-coverage model, ensuring that each tag is monitored by at least k readers, and solved it with the Plant Growth Simulation Algorithm (PGSA), which separates the treatment of objectives and constraints to enhance convergence stability. Hosseinzadeh et al. [36] employed a Takagi-Sugeno-Kang (TSK) fuzzy model for the deployment of RFID antennas, complemented by an offline hyper-parameter tuning phase using Greylag Goose Optimization (GGO). Additionally, Lamin et al. [37] introduced a fuzzy-guided Ant Colony Optimization (ACO) approach for sequential RFID network design in hospital environments, utilizing heterogeneous multi-port readers equipped with directional antennas.

2.4 Our Contributions

An examination of the existing RNP approaches indicates that heuristic-based methods are preferred due to their simplicity and rapid execution, which makes them well-suited for real-time applications.

However, they often lack global search capability and deliver suboptimal performance. In contrast, metaheuristic-driven methods provide greater flexibility and stronger exploration mechanisms, enabling more efficient optimization of the conflicting objectives inherent in multi-criteria RNP problems. From a network modeling perspective, the use of omnidirectional antennas typically results in excessive interference, while studies employing directional antennas often assume homogeneous antenna characteristics, overlooking variations in coverage behavior.

To address these limitations, the proposed KBGWO-RNP model embeds knowledge-based heuristic information (from structural and environmental factors) into the search process of the metaheuristic-driven GWO algorithm. By incorporating heuristic local search operators based on the network structure, the proposed model effectively guides the metaheuristic algorithm toward high-quality solutions with faster convergence. Furthermore, through supporting directional RFID antennas with heterogeneous configurations in terms of gain, read range, and beam width, the KBGWO-RNP framework achieves high coverage with minimal interference and deployment cost.

3 Network Model

The KBGWO-RNP framework builds upon [28,36,37] by extending traditional RNP models to account for the deployment cost of antennas and readers, and by supporting multi-port readers capable of hosting one or more directional antennas. In hospital environments, the presence of dense metallic equipment often renders omnidirectional antennas ineffective due to excessive interference. To mitigate this, the framework employs heterogeneous directional antennas, reducing overlap and interference between adjacent antenna footprints. Consequently, KBGWO-RNP aims not only to maximize network coverage but also to identify an optimal configuration that balances coverage, interference, and deployment cost.

The notations used throughout the paper are summarized in Table 1. Let us consider a hospital plan as an $M \times N$ grid, where each grid cell $g \in G$ (1 m × 1 m) can host an RFID reader supporting one or more directional antennas. This grid-based representation enables the formulation of zone criticality, wall positions, coverage, interference, cost, and other optimization parameters. The primary goal is to determine the optimal positioning and configuration of directional RFID antennas within the hospital layout, where each antenna is characterized by its type, read range, beam width, and orientation.

Table 1: Notations.

Indices	Definition
$i \in I$	Index of antennas
$j \in J$	Index of readers
$t \in T$	Index of types of antennas
$d \in D$	Index of antenna directions against X-axis
$m \in M$	Index of horizontal positions in the hospital plan
$n \in N$	Index of vertical positions in the hospital plan
$g \in G$	Index of all grids in the hospital plan
$w \in G$	Index of grids located on walls
Parameters	**Definition**
C_g	Criticality rate (%) of grid g
COV_g	1 if grid g is covered by at least one antenna; 0 otherwise
INT_g	1 if grid g is covered by more than one antenna; 0 otherwise
$MaxR$	The maximum read range of the different antennas, i.e., $MaxR = 10$
$H(g)$	Set of adjacent grids of central grid g within its $MaxR$
$V_{i,g,t,d,h}$	If grid h is within the coverage profile of antenna i with type t and direction d located at grid g

(Continued)

Table 1 (continued)

Indices	Definition
$B_{i,g,t,d,h}$	If grid h is interfered by the coverage profile of antenna i with type t and direction d located at grid g
$d_{i,g,t,d,w}$	Distance between wall w in the coverage profile of antenna i with type t and direction d located at grid g
R_t	Read range of an antenna with type t (based on Table 2)
COV_{min}	Minimum acceptable coverage level (%)
C_R	Cost of a reader
$A_{\max}$	Maximum number of antennas allowed in the network
Decision Variables	**Definition**
$P_A(i,g)$	1 if antenna i is placed at grid g; 0 otherwise: $X_A(i,g) \in \{0,1\}$
$X_A(i)$	Horizontal position on antenna i: $X_A(i) \in M$
$Y_A(i)$	Vertical position on antenna i: $Y_A(i) \in N$
$T(i)$	Type of antenna i: $T(i) \in T$
$D(i)$	Direction of antenna i: $D(i) \in D$
$G(i)$	Gain of antenna i
$R(i)$	Read range of antenna i
$B(i)$	Beam width of antenna i
$C(i)$	Normalized cost of antenna i
$P_R(j,g)$	1 if reader j is placed at grid g; 0 otherwise: $P_R(j,g) \in \{0,1\}$

As illustrated in Fig. 1, each antenna generates a fan-shaped radiation pattern, defined by a specific read range, beam width, and direction relative to the X-axis. Table 2 summarizes a library of 10 heterogeneous antenna models based on, used in KBGWO-RNP, all with circular polarization and distinct features such as read range, beam width, and cost. The maximum read ranges span 4–10 m, with two operational ranges considered based on full or 50% maximum gain, resulting in 20 different types of antennas. Beam widths vary from 40° to 115°, providing flexibility to meet diverse coverage requirements. In the RNP optimization process, KBGWO-RNP selects antenna types based on the coverage requirements and spatial characteristics of each area, achieving a balanced trade-off between extensive coverage, precise detection, and minimal interference.

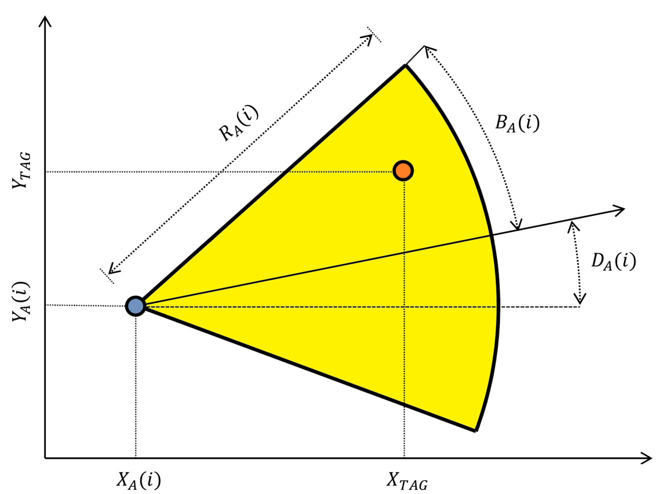

Figure 1: Directional modeling of antenna i with read range $X_A(i)$, beam width $B_A(i)$, and direction $D_A(i)$.

Table 2: Characteristics of directional RFID antennas used in the KBGWO-RNP model.

Antenna	$T(i)$: Type	Max. Range (m)	Cost ($)	$G(i)$: (dBi)	$R(i)$: (m)	$B(i)$	$C(i)$
Keonn P13	1 2	4	220$	3.45 6.9	2 4	90°	0.220
Keonn P11	3 4	5	190$	3.8 7.6	2.5 5	70°	0.190
Keonn P33	5 6	6	140$	4.8 9.6	3 6	40°	0.140
Times7 A4030	7 8	6	180$	3.25 6.5	3 6	60°	0.180
Times7 A6032	9 10	6	215$	3.5 7.0	3 6	75°	0.215
Keonn P12	11 12	8	220$	4.75 9.5	4 8	70°	0.220
Times7 A6034	13 14	9	190$	4.5 9.0	4.5 9	50°	0.190
Times7 A5010	15 16	9	235$	4 8	4.5 9	68°	0.235
Keonn P16	17 18	9	270$	4.65 9.3	4.5 9	90°	0.270
Times7 A5060	19 20	10	250$	5.25 10.5	5 10	60°	0.250

It is important to note that the adopted antenna model represents a planning-level abstraction, where directional coverage is approximated using geometric fan-shaped sectors and grid-based discretization. While this formulation does not explicitly capture complex electromagnetic phenomena such as multipath fading, diffraction, or material-dependent attenuation, it provides a computationally efficient and sufficiently accurate representation for solving RNP in hospitals.

4 Proposed KBGWO-RNP Framework

The goal of the proposed KBGWO-RNP framework is to obtain the optimal placement and configuration of directional RFID antennas across a hospital layout while satisfying a predefined minimum coverage requirement. The model jointly optimizes antenna positions, types, orientations, read ranges, and beam widths to achieve an effective trade-off among coverage, interference, and deployment cost. To address environmental constraints, walls are explicitly modeled as hard attenuation barriers that impose signal blocking constraints in the coverage evaluation process. These refinements enhance the environmental awareness of the optimization process without increasing the complexity of full electromagnetic simulation. Accordingly, the proposed framework is designed for optimization-level RNP, rather than detailed physical-layer RF modeling, which strengthens both the computational efficiency and applicability of the method in hospital environments.

The overall workflow of the KBGWO-RNP framework is illustrated in Fig. 2. The process starts with the generation of an initial population of candidate RNP solutions. It then enters an iterative optimization loop composed of three main stages. First, each solution is decoded and evaluated using a multi-criteria fitness function that reflects coverage, interference, and cost objectives. Next, the population is updated using the GWO algorithm, which balances exploration and exploitation by modeling social hierarchy and hunting behavior. Finally, a knowledge-based heuristic (i.e., KBH) is applied to refine promising solutions by incorporating structural and environmental information from the hospital layout. Each iteration executes these stages sequentially, and the optimization process continues until the predefined maximum number of iterations is reached, which serves as the termination criterion.

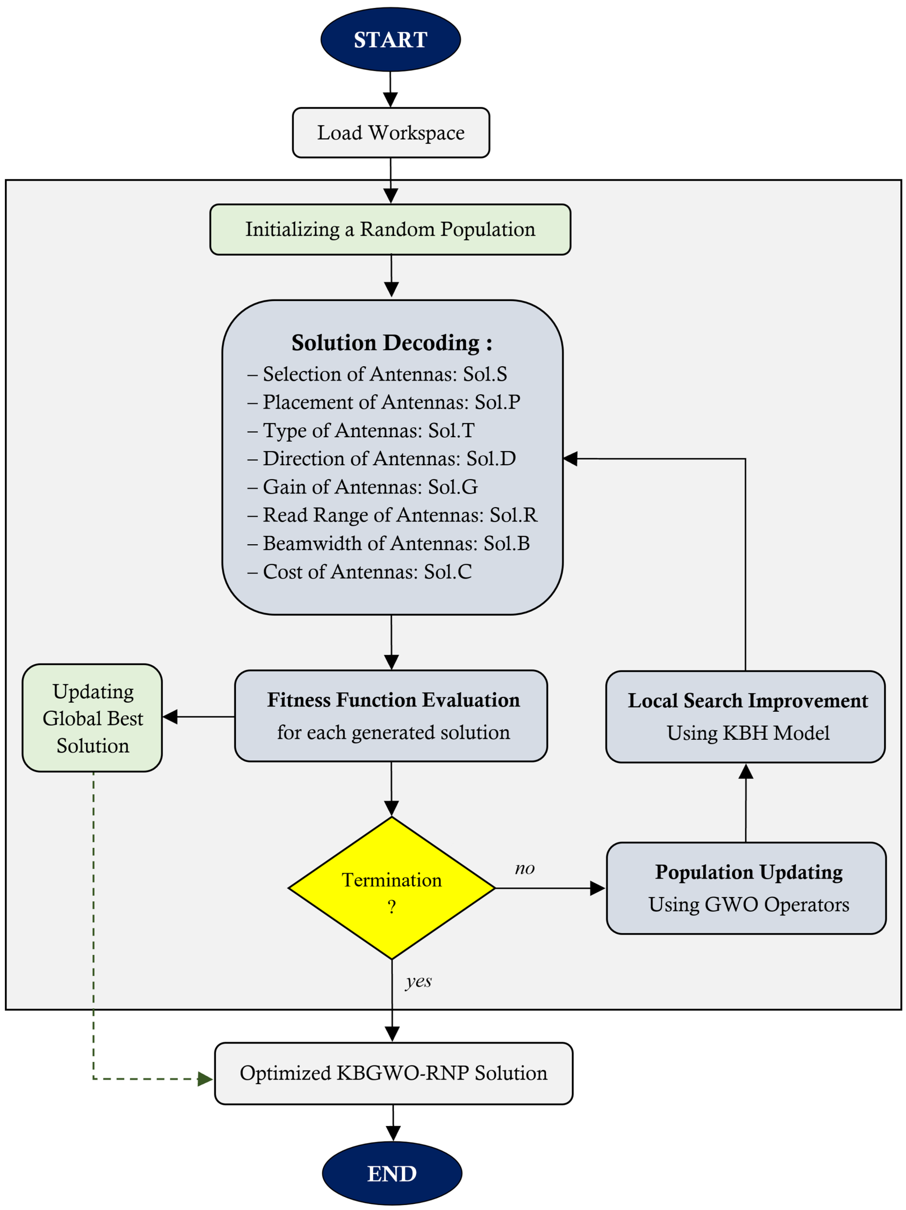

Figure 2: Overall flowchart of the KBGWO-RNP framework.

4.1 Problem Representation

As illustrated in Fig. 3, a feasible solution, denoted as Sol (i.e., a grey wolf), is represented by four direct and four indirect vectors, each of length A_{max}. Specifically, each solution is encoded using four direct sub-structures: a binary vector Sol.S, which indicates the selection or exclusion of antennas for deployment within the hospital layout, and three integer vectors Sol.G, Sol.T, and Sol.D, representing the grid location, antenna type, and orientation of each antenna, respectively.

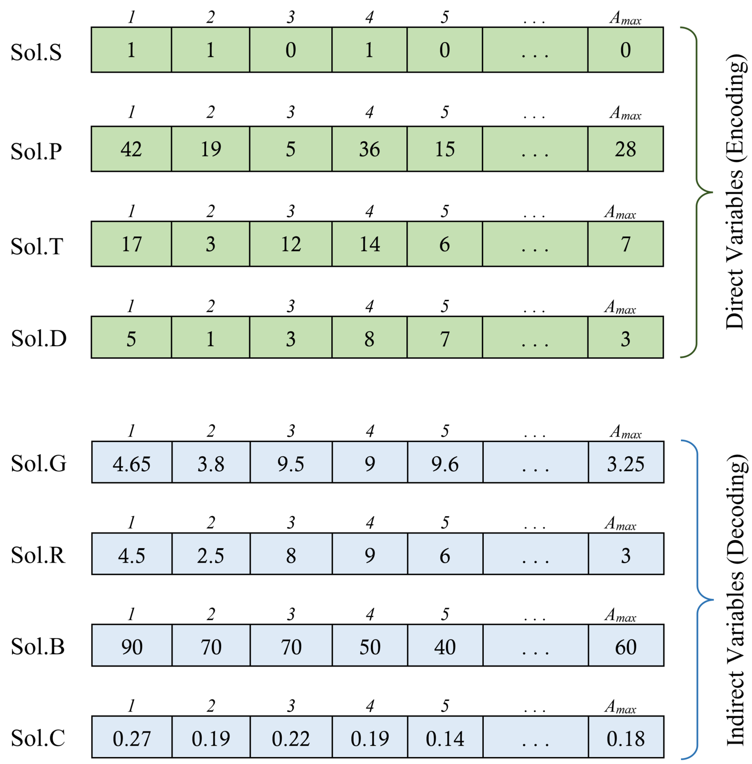

Figure 3: Representation of a feasible solution, i.e., encoding of a grey wolf.

Based on the selected antenna types (Sol.T) and their corresponding specifications listed in Table 2, the indirect variables including antenna gain (Sol.Ga), read range (Sol.R), beam width (Sol.B), and deployment cost (Sol.C), can be simply derived. These indirect variables are therefore implicitly determined by the direct encoding and do not require independent optimization variables. Accordingly, the direct variables used to encode each feasible solution in the KBGWO-RNP framework can be expresses as:

$$\mathrm{Sol.S}(i) = \begin{cases} 1 & \text{if antenna } i \text{ is selected} \\ 0 & \text{otherwise} \end{cases}, \tag{1}$$

$$\mathrm{Sol.P}(i) = \text{ selected grid for placement of antenna } i\text{: } \mathrm{Sol.P}(i) \in G, \tag{2}$$

$$\mathrm{Sol.T}(i) = \text{ selected type for antenna } i\text{: } \mathrm{Sol.T}(i) \in T, \tag{3}$$

$$\mathrm{Sol.D}(i) = \text{ selected direction for antenna } i\text{: } \mathrm{Sol.D}(i) \in D. \tag{4}$$

4.2 Fitness Function

The fitness function is designed to maximize the total criticality-weighted coverage (F_1) while minimizing the criticality-weighted interference (F_2) and the total deployment cost including reader and antenna costs (F_3). Generally, Pareto-based multi-objective optimization and weighted-average single-objective optimization are two common methods for handling multiple objectives, each with its own advantages and limitations depending on the problem requirements and decision-making context. In this paper, we utilize the weighted fitness formulation to provide controllable prioritization among the competing objectives while maintaining algorithmic simplicity and computational efficiency. Accordingly, objectives F_1, F_2, and F_3, are combined into a single-objective fitness function as follows:

$$\text{Fitness} = \text{maximize}\left\{w_1 \times F_1 + w_2 \times F_2 + w_3 \times F_3\right\}, \tag{5}$$

where w_1, w_2, and $w_3 \in [0, 1]$ ($w_1 + w_2 + w_3 = 1$) are the relative weights of the coverage, interference, and cost, within the total fitness function, respectively. These weights can be adjusted by the hospital decision-maker according to the specific application requirements and deployment priorities. Furthermore, the three sub-objectives F_1, F_2, and F_3 can be calculated as:

$$F_1 = \frac{\sum_{g=1}^{G} C_g \times COV(g)}{\sum_{g=1}^{G} C_g}, \tag{6}$$

$$F_2 = 1 - \frac{\sum_{g=1}^{G} C_g \times INT(g)}{\sum_{g=1}^{G} C_g}, \tag{7}$$

$$F_3 = 1 - \frac{\sum_{i=1}^{I}\sum_{g}^{G} Sol.C(i) \times P_A(i,g) + \sum_{j=1}^{J}\sum_{g}^{G} C_R \times P_R(j,g)}{\max(C) \times A_{\max} + C_R \times A_{\max}}, \tag{8}$$

Subject to:

$$F_1 \geq Cov_{min}, \tag{9}$$

$$\text{Sol.S}(i) \leq 1 \quad \forall i \in I, \tag{10}$$

$$\sum_{g=1}^{G} P_A(i,g) \leq 1 \quad \forall g \in G, \tag{11}$$

$$\sum_{g=1}^{G}\sum_{i=1}^{I} P_A(i,g) \leq A_{max}, \tag{12}$$

$$\sum_{j=1}^{J} P_R(j,g) \leq 1 \quad \forall g \in G, \tag{13}$$

$$\sum_{i=1}^{I} P_A(i,g) \leq 4 \quad \forall g \in G. \tag{14}$$

Eq. (9) enforces that the total coverage meets the minimum acceptable level. Eq. (10) specifies whether an antenna i is selected for deployment, while Eq. (11) ensures that each selected antenna is assigned to a specific grid location. Eq. (12) limits the total number of deployed antennas across the hospital layout to the maximum allowable value A_{max}. Eq. (13) restricts each grid location to at most one specific reader.

Finally, Eq. (14) constrains the number of antennas placed at any reader (grid) to 4, supporting single-, two-, and four-port reader configurations.

4.3 Population Updating Using GWO

Grey Wolf Optimizer (GWO) is a population-based metaheuristic that has proven effective for continuous optimization tasks by striking a strong balance between global exploration and local exploitation, while also exhibiting rapid convergence toward near-optimal solutions. GWO is characterized by a small number of control parameters, straightforward implementation, and competitive convergence speed [38,39], which make it attractive for complex optimization problems such as RNPs.

In the proposed KBGWO-RNP framework, the optimization process begins with a random initial population of grey wolves, where each wolf encodes a feasible RFID network design through four sub-solution components, namely Sol.S, Sol.P, Sol.T, and Sol.D, as depicted in Fig. 3. During each iteration of the algorithm, all candidate solutions are evaluated using the fitness function and then ranked in descending order. Then, the three highest-quality grey wolves are identified as the X_α (alpha), X_β (beta), and X_δ (delta) wolves, as follows:

$$X_1(k) = X_\alpha - A_1 \cdot |C_1 X_\alpha - X_{OLD}(k)|, \tag{15}$$

$$X_2(k) = X_\beta - A_2 \cdot |C_2 X_\beta - X_{OLD}(k)|, \tag{16}$$

$$X_3(k) = X_\delta - A_3 \cdot |C_3 X_\delta - X_{OLD}(k)|. \tag{17}$$

The remaining wolves update their positions based on the guidance of these three leaders using the position update rule in Eq. (18). In this mechanism, the coefficient vectors $A_{1,2,3}$ and $C_{1,2,3}$ are calculated as $A = 2a{\cdot}r_1 - a$ and $C = 2r_2$, respectively, where r_1 and r_2 are random vectors with values within $[0, 1]$, and a is a linearly decreasing parameter that transitions from 2 to 0 throughout the optimization process.

$$X_{NEW}(k) = \frac{(X_1(k) + X_2(k) + X_3(k))}{3}. \tag{18}$$

Based on these update equations, wolves move toward promising regions of the search space when $|A| < 1$ (attacking prey), corresponding to exploitation, and explore new regions when $|A| > 1$ (search for prey). With the progression of iterations and the gradual decrease of a, the search shifts from exploration to exploitation, enabling efficient solution refinement and convergence to high-quality RNP configurations.

4.4 Local Search Improvement Using KBH

To strengthen the search capability of GWO within the KBGWO-RNP framework, a KBH-based local search improvement phase is applied to each grey wolf. The proposed KBH is considered knowledge-based because it integrates multiple sources of domain-specific and structural knowledge (i.e., coverage demand, interference interactions, and environmental constraints) and aggregates them into a multi-criteria heuristic model that dynamically adapts to the current state of the network. Although the KBH introduces a guided local search mechanism, it does not lead to premature convergence due to the concurrent exploration capability of the GWO population. The hybrid design preserves diversity while enabling informed refinement, thereby mitigating the risk of stagnation in local optima.

As illustrated in Pseudo-code of Algorithm 1 and Fig. 4, the KBH algorithm exploits structural and environmental knowledge through three context-aware input parameters to assess the suitability of candidate modifications for a randomly selected antenna in each solution. The first input $H_1(i, g, t, d)$ represents the coverage density obtained by placing antenna i at grid g with type t and direction d to cover currently uncovered grids. This metric evaluates the concentration of critical grids within the coverage footprint of the antenna and favors antenna configurations that maximize coverage of high-priority or densely populated tag areas. By steering directional beams toward regions with greater unmet demand (non-covered grids), this input promotes efficient utilization of antenna resources. It is formulated as follows:

$$H_1(i,g,t,d) = \frac{\sum_{h\in H(g)} \left(C_h \times (1 - COV_h) \times V_{i,g,t,d,h}\right)}{\sum_{h\in H(g)} C_h}. \tag{19}$$

The second input $H_2(i,g,t,d)$ denotes the inter-antenna interference associated with antenna i when deployed with type t and direction d. This parameter enables a balanced trade-off between coverage expansion and interference mitigation by penalizing configurations that introduce excessive overlap with already deployed antennas. Consequently, antenna placements with lower mutual interference are preferred to be selected. This input can be computed as follows:

$$H_2(i,g,t,d) = \frac{\sum_{h\in H(g)} \left(C_h \times COV_h \times B_{i,g,t,d,h}\right)}{\sum_{h\in H(g)} C_h}. \tag{20}$$

The third input $H_3(i,g,t,d)$ captures the directional distance to walls for antenna i located at grid g under a given type and orientation. It measures the proximity of the main lobe of the antenna to the closest wall, reflecting the impact of physical obstructions on signal propagation. Since walls act as natural boundaries that can limit effective coverage and cause energy loss, antenna orientations pointing directly toward nearby walls are penalized. This encourages beam directions that better exploit effective open spaces and improve coverage efficiency in indoor hospital environments. The formulation is given by:

$$H_3(i,g,t,d) = \frac{\min_w \left(d_{i,g,t,d,w}\right)}{R_t}. \tag{21}$$

After calculating the three input parameters for all candidate modifications for antenna i, the KBH-based score of each candidate is calculated. The higher values of H_1 and H_3 increase the score, whereas lower values of H_2 are favored to reduce interference. Since all three inputs are normalized within the range $[0,1]$ using Eqs. (19)–(21), they can be merged to calculate the KBH-based score as follows:

$$S(i,g,t,d) = \alpha_1 \times H_1(i,g,t,d) + \alpha_2 \times (1 - H_2(i,g,t,d)) + \alpha_3 \times H_3(i,g,t,d), \tag{22}$$

where α_1 to α_3 are weighting coefficients in $[0,1]$ satisfying $\alpha_1 + \alpha_2 + \alpha_3 = 1$, allowing flexible control over the relative importance of coverage, interference, and wall-awareness in the local search decision process, while considering the correlations with already deployed antennas.

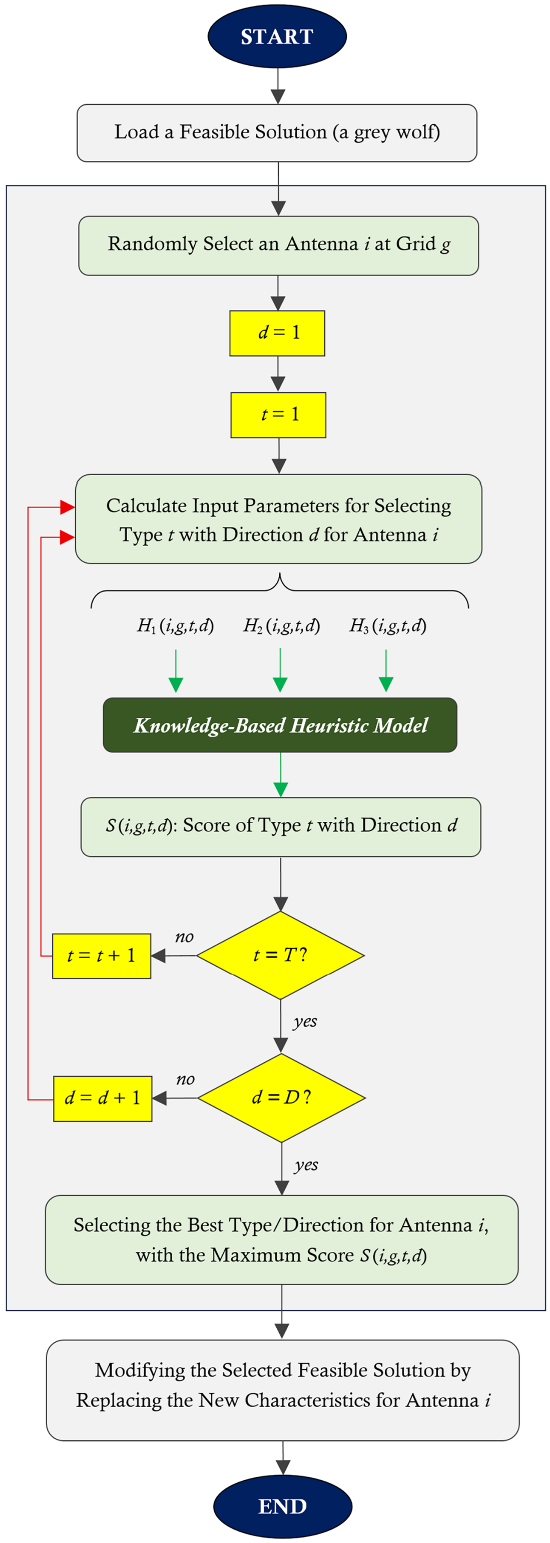

Figure 4: Flowchart of local search improvement using the KBH model.

Algorithm 1: Pseudo-code of the KBH algorithm

Inputs:
Current solution X
Workspace G with criticality values
Antenna configuration (positions, types, directions)
Weights of the fitness functions
Weights of the KBH sub-heuristics
Output:
Improved solution X*
Begin
1: Evaluate current solution X:
  Compute coverage map
  Compute interference map
2: For each antenna i in X do
3:   Identify candidate modifications:
    -Change antenna direction
    -Change antenna position (local neighborhood)
    -Change antenna type (optional)
4:   For each candidate modification m do
5:     Apply modification m → generate new solution X^{new}
6:     Compute heuristic components:
      H_1 ← normalized uncovered criticality density
      H_2 ← normalized interference (overlap penalty)
      H_3 ← normalized wall-distance penalty
7:     Compute KBH score:
      $\text{Score}(m) = H_1 + H_2 + H_3$
8:   End For
9:   Select best modification m^* with minimum Score
10:   If Score(m^*) associated with X* improves current solution X then
    Update antenna i using X*
  End If
11: End For
12: Return improved solution X*
End

4.5 Computational Complexity Analysis

The time complexity of the KBGWO-RNP model can be analyzed by considering its two main components: the knowledge-based heuristic (KBH) and the Grey Wolf Optimizer (GWO). The KBH module performs local search refinement on each solution at every iteration. As illustrated in Fig. 4, it evaluates $T \times D$ candidate situations, resulting in a time complexity of $O(T \times D)$. Furthermore, the overall complexity of the GWO-based optimization process can be represented as $O\left(PopSize \times MaxIter \times \left(D_{GWO} + D_{KBH}\right)\right)$, where *PopSize* and *MaxIter* are the population size and the maximum iterations of GWO, respectively. Since the GWO-related complexity can be defined based on the number of grids and maximum deployable antennas as $D_{GWO} = G \times A_{max}$, the total time complexity of KBGWO-RNP is $O\left(PopSize \times MaxIter \times \left(G \times A_{max} + T \times D\right)\right)$.

Typically, both G and A_{max} are much larger than T and D, leading $G \times A_{max} >> T \times D$. It means that the computational cost of the KBH module per iteration and per solution can be dominated by that of the GWO component. Therefore, the overall time complexity of KBGWO-RNP can be reasonably simplified to $O\left(PopSize \times MaxIter \times G \times A_{max}\right)$. This analysis shows that, despite its effectiveness in improving solution quality and convergence speed, integrating the KBH module into the GWO search process adds only marginal overhead and does not significantly affect the overall computational complexity.

5 Simulation Analysis

The proposed model was implemented in MATLAB R2024b, with simulations run on a desktop featuring an Intel Core i7-6700HQ 2.5 GHz processor and 16 GB RAM.

5.1 Settings

To evaluate the performance of the KBGWO-RNP model, we applied it to a hospital plan, with randomly assigned criticality levels across the grid. The hospital plan, shown in Fig. 5, reflects an indoor healthcare environment characterized by corridors, walls, and heterogeneous patterns of medical asset occurrence. To assess the performance of the KBGWO-RNP framework, a simulated indoor workspace was configured as summarized in Table 3. The environment covers an area of 40 m × 20 m, discretized into 1 m × 1 m grid cells, resulting in a total of 800 grids. Within this space, up to 50 directional RFID antennas can be deployed at accessible grids. As described in Section 3, a library of 20 heterogeneous antenna types is used, each characterized by different gain, read range, beam width, and cost. The read ranges are from 2 to 10 m, while the beam widths span 40° to 90°, offering flexible options to meet the different coverage requirements.

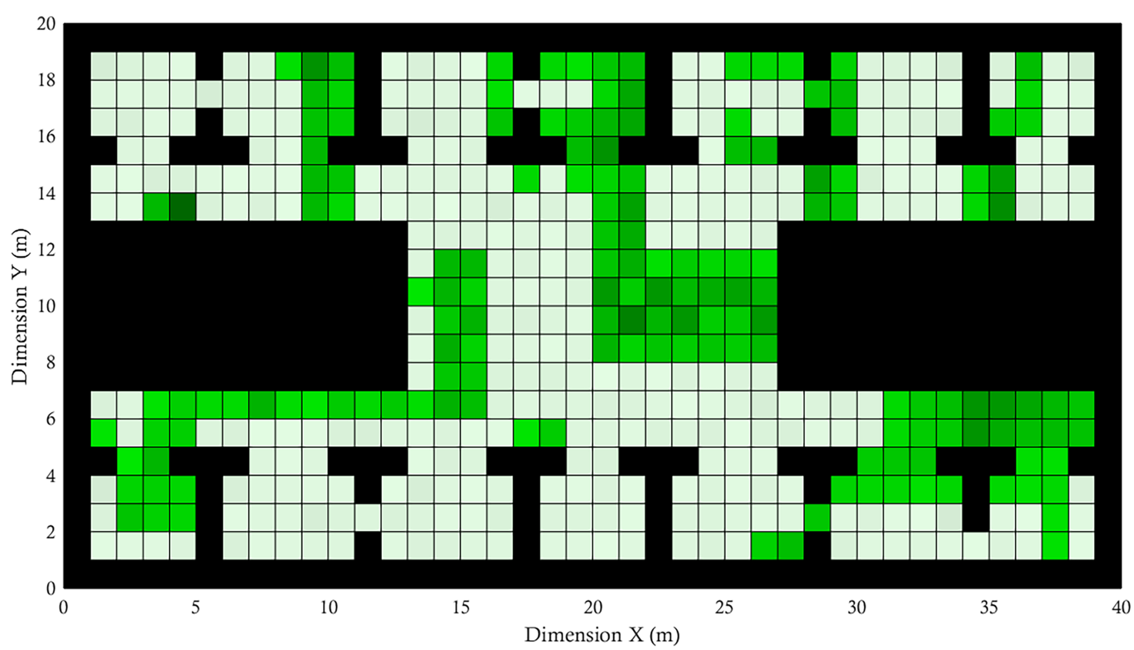

Figure 5: Grid-based hospital layout with the reference criticality map, showing walls (black cells) and accessible areas (green cells) with varying criticality levels (darker green indicates higher criticality).

Table 3: Network parameters.

Parameter	Value
Network dimension	40×20
Number of grids (G)	800
Size of each grid	1 m × 1 m
Maximum allowable antennas (A_{max})	25
Number of antenna types (T)	20
Number of antenna directions (D)	8
Antenna directions: $D(i)$	$\{0, 45, 90, 135, 180, 225, 270, 325\}$
Gain rate of antennas	$\{50, 100\}$%
Gain of antennas: $G(i)$	[3.25, 10.5] dBi
Read range of antennas: $R(i)$	[2, 10] m
Beamwidth of antennas: $B(i)$	[40, 90]°
Typical cost of antennas	[140, 270]$
Normalized cost of each antenna: $C(i)$	[0.14, 0.27]
Typical cost of each reader	1000$
Normalized cost of each reader: C_R	1

Furthermore, Table 4 lists the controllable parameters of KBGWO-RNP. The population size of GWO is set to 20, and the number of iterations is 300. The three KBH input parameters are assigned equal influence. For the fitness function, the weights are set to $w_1 = 0.25$, $w_2 = 0.25$, and $w_3 = 0.5$, assigning half of the total weight to deployment cost and the remaining half to balancing performance metrics: i.e., coverage and interference. Moreover, the minimum acceptable coverage rate is set to 60%, 75%, and 90%.

Table 4: KBGWO-RNP parameters.

Parameter	Value
Population of GWO ($PopSize$)	20
Iterations of GWO ($MaxIter$)	300
Influence of coverage in the fitness function (w_1)	0.25
Influence of interference in the fitness function (w_2)	0.25
Influence of cost in the fitness function (w_3)	0.5
Weights of the KBH model (α_1 to α_3)	1/3
Minimum acceptable coverage (COV_{min})	$\{60, 75, 90\}$%

In Section 5.2, the performance of the KBGWO-RNP model is evaluated under different scenarios with varying values of COV_{min}, while keeping the fitness function weights fixed at $w_1 = 0.25$, $w_2 = 0.25$, and $w_3 = 0.5$. In Section 5.3, the KBGWO-RNP approach is compared against existing methods reported in the literature to demonstrate its relative effectiveness. Sections 5.4, 5.5, and 5.6 present a series of sensitivity analyses to investigate the impact of key parameters, including the minimum acceptable coverage rate, the fitness function weights, and the structure of the criticality maps, respectively. In Section 5.7, a statistical analysis is conducted using randomly generated criticality maps to assess the robustness and stability of the proposed approach under varying spatial conditions. Finally, an ablation study is presented in Section 5.8 to evaluate the contribution of the individual components of the KBGWO-RNP framework.

It should be noted that the main comparative results presented in Sections 5.2 to 5.5 correspond to representative executions under the same reference map configuration (as seen in Fig. 5), while the analyses reported in Sections 5.6 to 5.8 primarily evaluate robustness against spatial criticality variability across different generated maps.

5.2 Results of KBGWO-RNP

In this section, the results of the KBGWO-RNP framework for three scenarios considering COV_{min} as 60% (Scenario C1), 75% (Scenario C2), and 90% (Scenario C3), are reported. The results obtained for Scenario C1 (COV_{min} = 60%) demonstrate the capability of KBGWO-RNP to achieve acceptable coverage with a very compact and cost-efficient deployment. As shown in Fig. 6, the algorithm rapidly converges to a stable solution, reaching a fitness value of 0.824 within 200 iterations. As shown in Table 5 and Fig. 7, only six antennas and four readers are deployed, while maintaining extremely low interference. This behavior reflects the effectiveness of the KBH component in guiding antenna placement toward high-criticality regions while avoiding unnecessary overlaps. In this scenario, the optimizer prioritizes strategic placement rather than extensive deployment, resulting in a low normalized cost and a high overall fitness value.

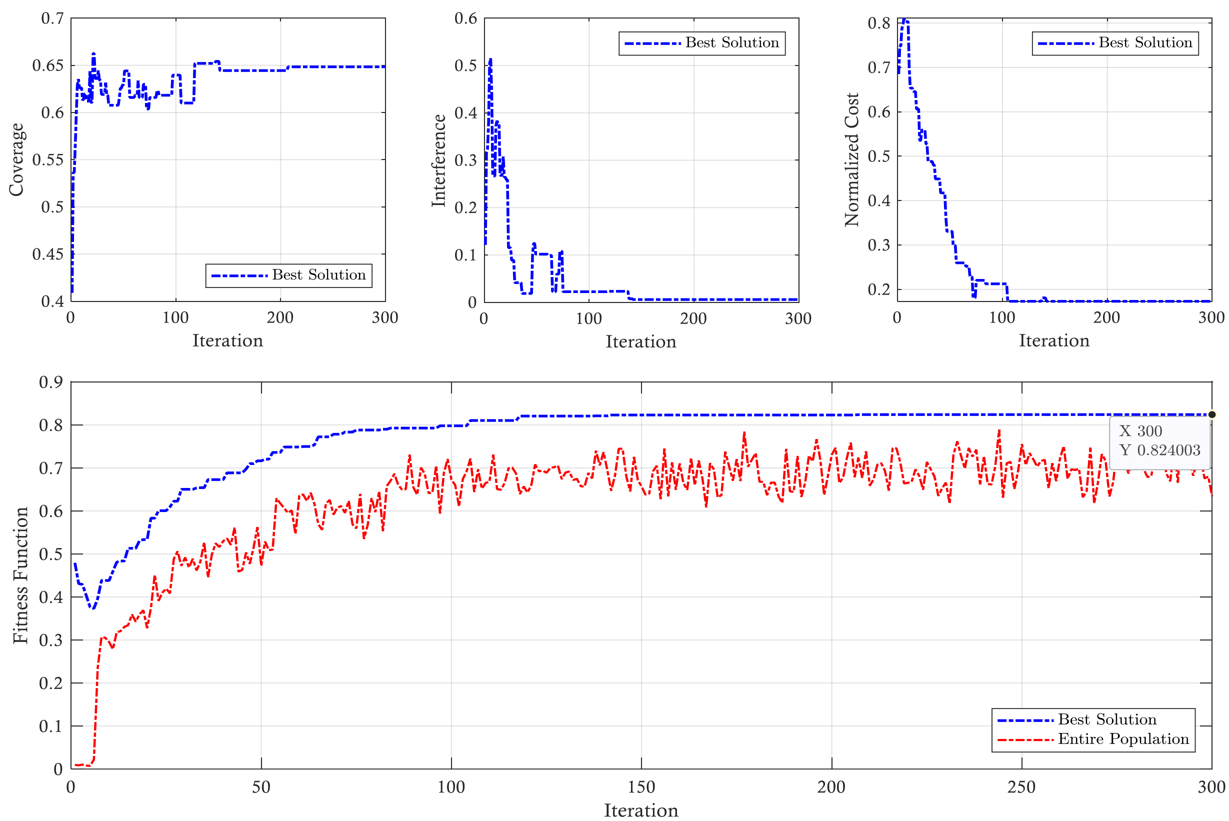

Figure 6: Convergence graphs of KBGWO-RNP for scenario C1: coverage (top left), interference (top middle), cost (top right), and fitness function (bottom).

Table 5: Detailed results of KBGWO-RNP for scenario C1 (COV_{min} = 60%, w_1 = 0.25, w_2 = 0.25, and w_3 = 0.5).

Antenna	X (m)	Y (m)	Type #	Gain (dBi)	Orientation	Beamwidth	Range (m)	Cost ($)
1	14	19	18	9.3	225	90	9	270
2	30	4	20	10.7	0	60	10	250
3	23	12	18	9.3	225	90	9	270
4	23	12	16	8	315	68	9	235
5	23	12	18	9.3	90	90	9	270
6	2	4	20	10.7	45	60	10	250

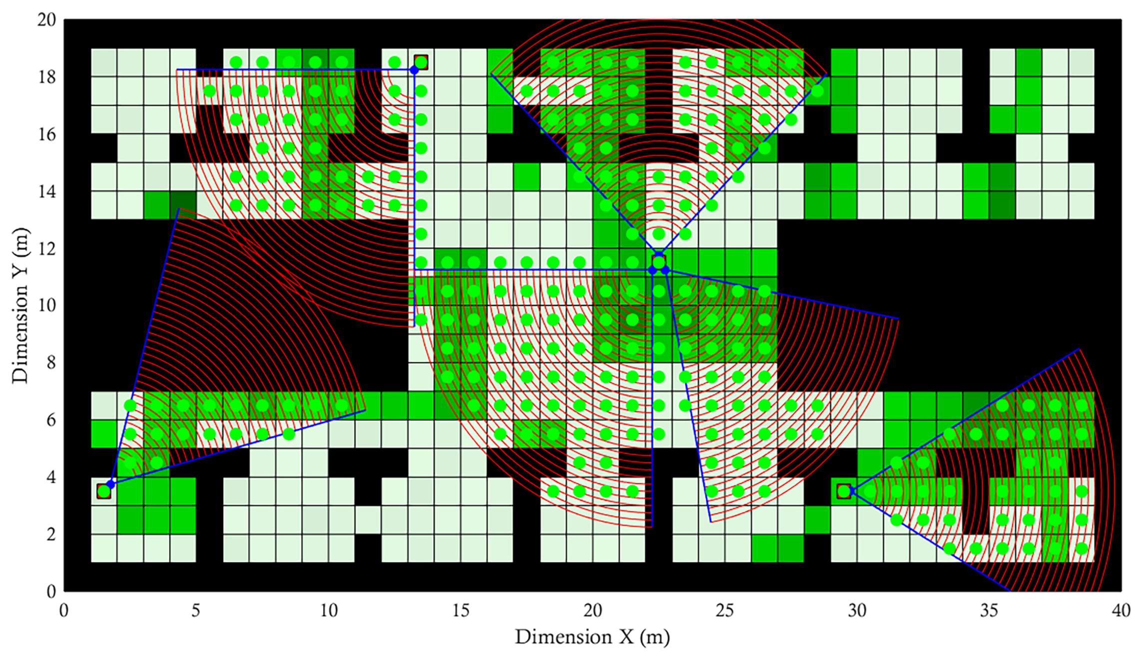

Figure 7: Graphical representation of KBGWO-RNP for scenario C1.

As COV_{min} increases to 75% in Scenario C2, the algorithm naturally shifts toward a denser deployment strategy. The number of antennas and readers increases to satisfy the stricter coverage requirement, as reflected in Table 6 and Fig. 8. Importantly, the growth in interference remains controlled, which highlights the role of directional antennas and interference knowledge-based rules embedded in KBH. Instead of uniformly increasing transmission power or beam width, the algorithm selects heterogeneous antenna types and orientations to selectively expand coverage while limiting overlap.

Table 6: Detailed results of KBGWO-RNP for scenario C2 (COV_{min} = 75%, w_1 = 0.25, w_2 = 0.25, and w_3 = 0.5).

Antenna	X (m)	Y (m)	Type #	Gain (dBi)	Orientation	Beamwidth	Range (m)	Cost ($)
1	21	12	18	9.3	180	90	9	270
2	21	3	14	9	180	50	9	190
3	21	3	10	7	90	75	6	215
4	21	3	20	10.5	45	60	10	250
5	15	16	12	9.5	180	70	8	220
6	15	16	2	6.9	45	90	4	220

(Continued)

Table 6 (continued)

Antenna	X (m)	Y (m)	Type #	Gain (dBi)	Orientation	Beamwidth	Range (m)	Cost ($)
7	19	18	16	8	315	68	9	235
8	7	7	15	4	0	68	4.5	235
9	7	7	18	9.3	225	90	9	270
10	33	18	8	6.5	180	60	6	180
11	32	15	18	9.3	0	90	9	270
12	32	15	11	4.75	180	70	4	220
13	34	6	10	7	0	75	6	215
14	34	6	2	6.9	180	90	4	220
15	34	6	13	4.5	45	50	4.5	190

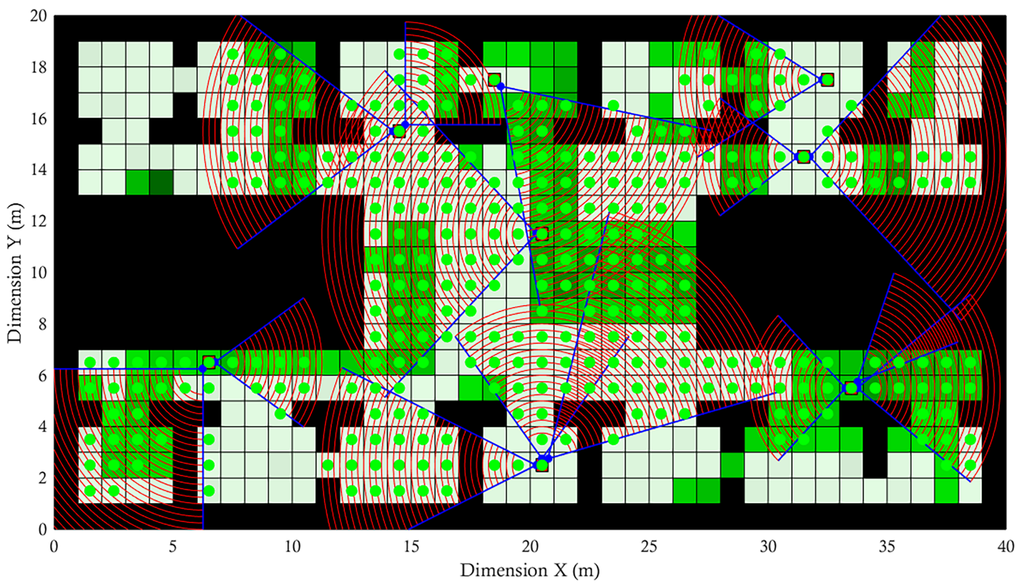

Figure 8: Graphical representation of KBGWO-RNP for scenario C2.

Scenario C3 (COV_{min} = 90%) represents a more challenging planning condition, requiring near-complete coverage of the hospital space. The results in Table 7 and Fig. 9 show that KBGWO-RNP meets this requirement by deploying 21 antennas across 14 readers, achieving over 90% coverage. As expected, higher coverage leads to increased interference and cost. These results confirm that KBGWO-RNP adapts its deployment strategy based on coverage demands, rather than relying on uniform or overly conservative configurations.

5.3 Comparison of KBGWO-RNP with Existing Methods

To evaluate the performance of the proposed KBGWO-RNP model, its results are compared against those obtained using HNRNPO [19], RNPPSO [32], and I-RAENNA [33]. All methods are evaluated under the same experimental environment, including the same hospital layout, discretized grid representation, grid resolution, and criticality map #1 (as illustrated in Fig. 5). All approaches employ the same antenna library consisting of 20 heterogeneous directional antenna types, as well as identical deployment cost parameters for antennas and readers, as specified in Table 3. Furthermore, all compared metaheuristics were executed using the same population size of 300 and the same maximum number of iterations of 20.

Table 7: Detailed results of KBGWO-RNP for scenario C3 (COV_{min} = 90%, w_1 = 0.25, w_2 = 0.25, and w_3 = 0.5).

Antenna	X (m)	Y (m)	Type #	Gain (dBi)	Orientation	Beamwidth	Range (m)	Cost ($)
1	13	14	14	9	45	50	9	190
2	27	18	10	7	315	75	6	215
3	27	18	16	8	0	68	9	235
4	4	6	17	4.65	225	90	4.5	270
5	4	6	12	9.5	0	70	8	220
6	28	17	20	10.5	225	60	10	250
7	18	10	4	7.6	180	70	5	190
8	26	17	16	8	135	68	9	235
9	24	11	18	9.3	315	90	9	270
10	24	11	14	9	225	50	9	190
11	24	13	14	9	180	50	9	190
12	24	13	19	5.25	135	60	5	250
13	32	4	14	9	225	50	9	190
14	7	14	18	9.3	180	90	9	270
15	12	7	5	4.8	0	40	3	140
16	12	7	18	9.3	270	90	9	270
17	37	16	11	4.75	315	70	4	220
18	37	16	11	4.75	225	70	4	220
19	37	16	2	6.9	90	90	4	220
20	39	3	18	9.3	135	90	9	270
21	14	13	18	9.3	135	90	9	270

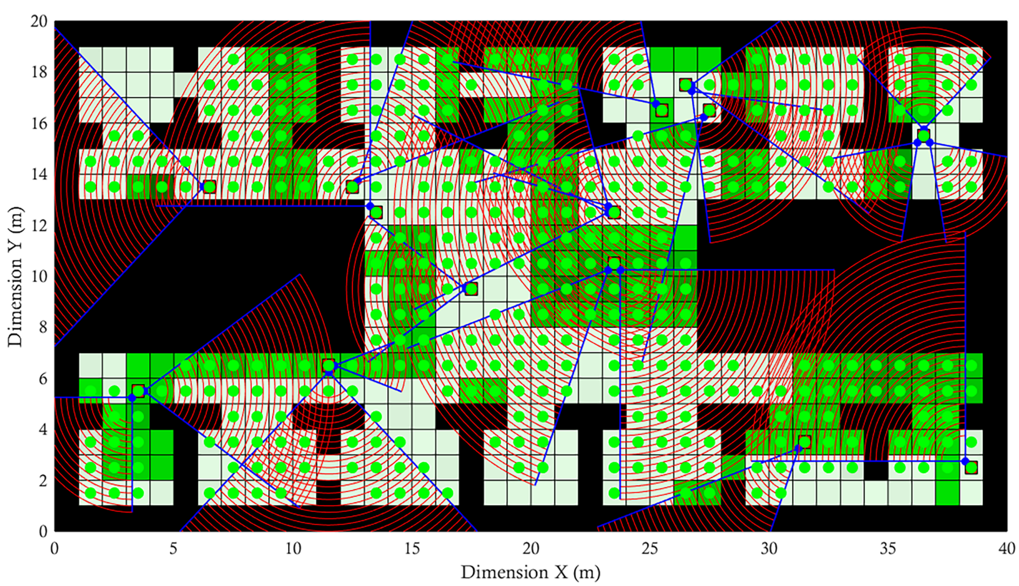

Figure 9: Graphical representation of KBGWO-RNP for scenario C3.

It should be noted that the proposed KBGWO-RNP framework explicitly incorporates a strict minimum coverage constraint (COV_{min} = 90% in Scenario C3), whereas the compared baseline methods were not originally designed with native hard-constraint handling mechanisms for minimum coverage enforcement. Therefore, exact equivalence between the constrained optimization formulation of KBGWO-RNP and the unconstrained behavior of the baseline methods cannot be fully guaranteed. To maintain approximate functional comparability among the evaluated methods and avoid clearly infeasible low-coverage deployments, only baseline solutions achieving coverage levels close to 90% were considered in the comparative analysis. It should be noted that this filtering criterion was introduced as a practical approximation rather than a strict equivalence condition.

Despite these methodological differences, the comparative results in Table 8 and Fig. 10 show that the proposed KBGWO-RNP framework achieves a more balanced trade-off among coverage, interference, and deployment cost. Although all methods produce relatively high coverage levels close to 90%, KBGWO-RNP achieves this performance with significantly lower cost and competitive interference levels. This improvement is primarily attributed to the integration of knowledge-based local refinement with the global exploration capability of GWO, in addition to the explicit modeling of heterogeneous directional antennas and multi-port reader deployment.

Table 8: Comparison of the results of KBGWO-RNP with existing methods.

Metric	HNRNPO [19]	RNP-PSO [32]	IRAENNA [33]	KBGWO-RNP
Number of antennas	22	21	19	21
Coverage (%)	86.7	88.9	90.7	90.4
Interference (%)	18.3	24.6	22.4	19.9
Cost ($)	27,500	26,250	23,750	18,775
Fitness function	0.488	0.497	0.547	0.631

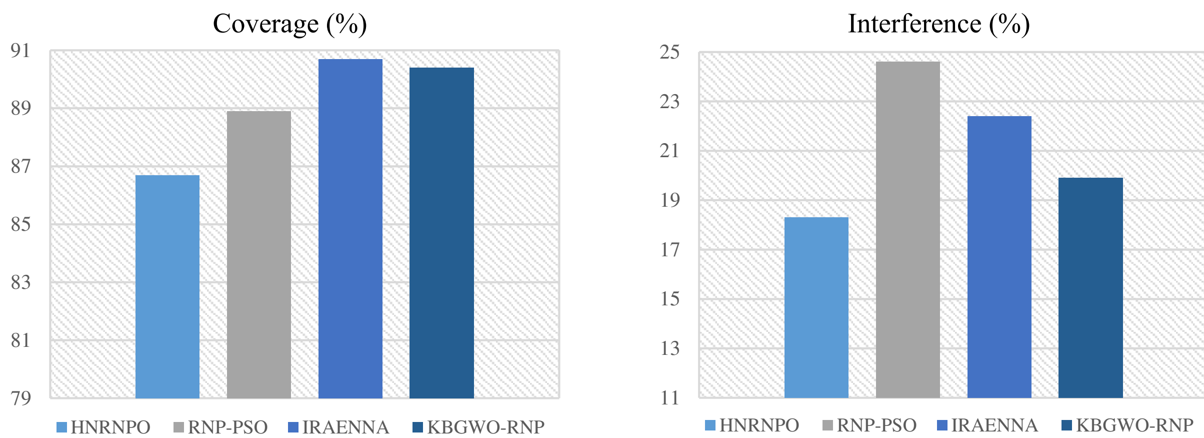

Figure 10: (Continued)

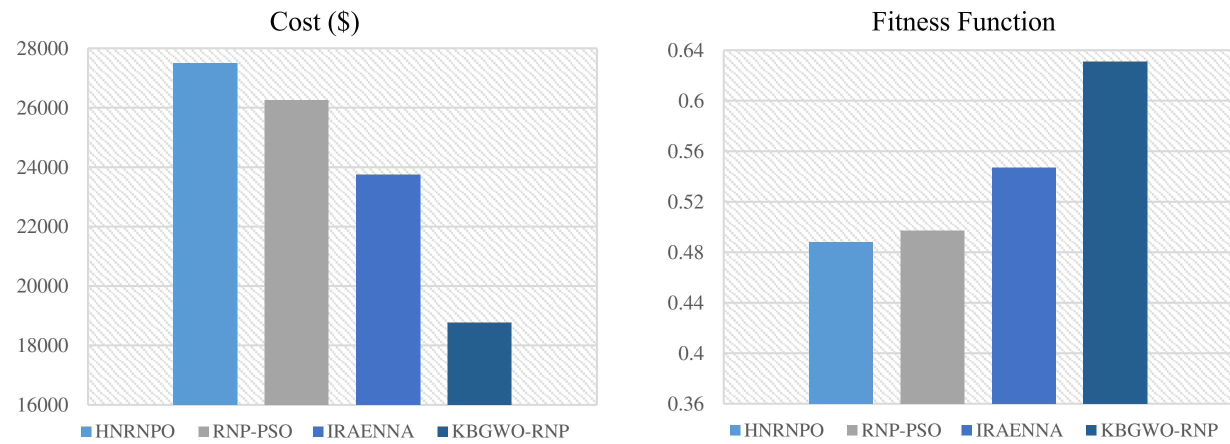

Figure 10: Comparison of the different methods in terms of coverage, interference, cost, and overall fitness function.

The improvement rates of the KBGWO-RNP model over the compared techniques are summarized in Table 9, where "+" indicates improvement and "−" denotes that the compared method performs better for the corresponding metric. Although KBGWO-RNP achieves slightly lower coverage than IRAENNA and slightly higher interference than HNRNPO, the proposed framework consistently provides the best overall fitness performance. Specifically, it achieves fitness improvements of up to 29.3% over HNRNPO, 27.0% over RNP-PSO, and 15.4% over IRAENNA. The comparative analysis suggests that embedding heuristic knowledge within a metaheuristic optimization framework can effectively guide the search toward more balanced and computationally efficient RNP configurations.

Table 9: Performance gain of the KBGWO-RNP model against existing methods.

Metric	vs. HNRNPO [19]	vs. RNP-PSO [32]	vs. IRAENNA [33]
Coverage	+4.2%	+1.7%	−0.33%
Interference	−8.7%	+19.1%	+11.7%
Cost	+31.7%	+28.5%	+20.9%
Fitness function	+29.3%	+27.0%	+15.4%

5.4 Sensitivity Analysis of Minimum Coverage Rate

In this section, a sensitivity analysis is conducted to evaluate the impact of the minimum acceptable coverage rate on the system's performance. Specifically, COV_{min} is varied across three levels as 60%, 75%, and 90%, corresponding to Scenarios C1, C2, and C3, respectively. This variation allows for a systematic examination of how stricter or more relaxed coverage requirements affect the resulting deployment strategy and overall solution quality. In addition, the analysis highlights the trade-offs that emerge among key performance dimensions, including coverage, interference, and cost, as the constraint becomes more demanding.

The sensitivity analysis presented in Table 10 and Fig. 11 provides an insight into how increasing the minimum acceptable coverage constraint (COV_{min}) impacts the trade-off between coverage, interference, and cost. It should be mentioned that the fitness function values are computed using the formulation defined in Eq. (5), where the overall fitness is expressed as a weighted sum of three sub-objectives: coverage, interference, and cost. Specifically, coverage is directly considered as a normalized fraction (F_1), while interference (F_2) and cost (F_3) are transformed into maximization terms by taking their complements, i.e., $F_2 = 1 -$ Interference (%) and $F_3 = 1 -$ Cost (%), since lower values are preferred for both metrics. After converting all percentage values into normalized form, the corresponding weights are applied to each component, and the final fitness value is obtained accordingly.

Table 10: Comparing the results of KBGWO-RNP in different scenarios.

Metric	C1 (COV_{min} = 60%)	C2 (COV_{min} = 75%)	C3 (COV_{min} = 90%)
Number of antennas	6	15	21
Number of readers	4	8	14
Cost of antennas ($)	1545	3400	4775
Cost of readers ($)	4000	8000	14,000
Total cost ($)	5545	11,400	18,775
Coverage (%)	64.8	77.5	90.4
Interference (%)	0.6	5.9	19.9
Cost (%)	17.4	35.9	59.1
F_1	0.648	0.775	0.904
F_2	0.994	0.941	0.801
F_3	0.826	0.641	0.409
Fitness function	0.824	0.749	0.631

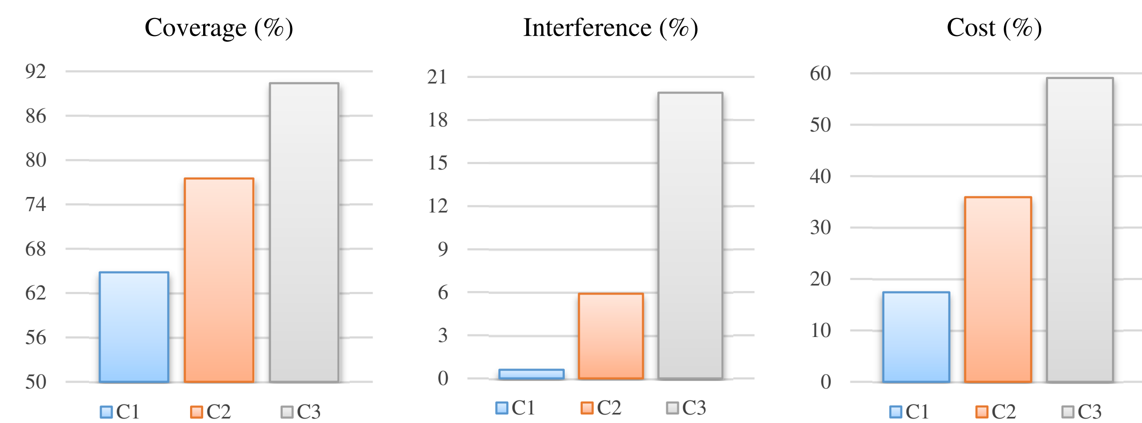

Figure 11: Comparison of the sub-objectives for different scenarios with the minimum acceptable coverage rate as 60% (scenario C1), 75% (scenario C2), and 90% (scenario C3).

As the required coverage rises from 60% to 90%, the model responds by gradually increasing the number of deployed antennas and readers. This behavior is consistent with fundamental RFID planning principles: higher coverage in indoor hospital environments requires more spatially distributed antennas to overcome walls, obstructions, and corridor segmentation. A key observation is the nonlinear increase in interference as coverage constraints become stricter: it is negligible in Scenario 1 but rises in Scenarios C2 and C3 due to denser deployments and overlapping radiation footprints. This growth is effectively moderated by the use of directional antennas and the interference-aware KBH parameter (H_2), which adapt beamwidths, directions, and gains to limit overlap and maintain acceptable signal quality even at higher coverage levels. It should be mentioned that the decreasing trend of the overall fitness value with higher coverage constraints does not indicate poorer performance, but rather reflects the stricter optimization conditions from Scenario C1 to Scenario C3.

5.5 Sensitivity Analysis of Fitness Function Weights

In this subsection, the sensitivity of the KBGWO-RNP model to different configurations of the fitness function weights is analyzed for Scenario C2 (COV_{min} = 75%), with a detailed focus on their impact on coverage, interference, cost, and the resulting fitness value. This analysis provides insight into how shifting the relative importance of the objectives influences the deployment strategy and overall solution quality.

Table 11 summarizes the results obtained under various weight combinations. Under the default configuration ($w_1 = 0.25$, $w_2 = 0.25$, $w_3 = 0.5$), the model achieves a well-balanced solution with 77.5% coverage, 5.9% interference, and 35.9% cost, resulting in a fitness value of 0.749. This confirms that prioritizing cost while maintaining moderate emphasis on coverage and interference leads to a strong overall trade-off. When the importance of interference is increased ($w_2 = 0.5$), the model reduces interference to 4.5%, indicating effective avoidance of overlapping coverage regions. However, this reduction comes at the expense of slightly lower coverage (76.2%) and higher cost (37.5%), leading to a decrease in fitness (0.728). This reflects the trade-off between minimizing interference and maintaining efficient coverage. In the next case, increasing the weight of coverage ($w_1 = 0.5$) improves coverage to 80.9%, but also results in higher interference (9.2%) and cost (39.1%). In this case, the fitness value rises to 0.758, suggesting that moderate emphasis on coverage can improve overall performance when balanced against the other objectives.

Table 11: Effects of the fitness function weights on the results of KBGWO-RNP for scenario C2 (COV_{min} = 75%).

Weights of Fitness Function	Coverage (%)	Interference (%)	Cost (%)	Fitness Value
$w_1 = 0.25$, $w_2 = 0.25$, $w_3 = 0.5$ (Default Weights)	77.5	5.9	35.9	0.749
$w_1 = 0.25$, $w_2 = 0.5$, $w_3 = 0.25$	76.2	4.5	37.5	0.728
$w_1 = 0.5$, $w_2 = 0.25$, $w_3 = 0.25$	80.9	9.2	39.1	0.758
$w_1 = 0.1$, $w_2 = 0.1$, $w_3 = 0.8$	75.8	6.8	33.1	0.733
$w_1 = 0.1$, $w_2 = 0.8$, $w_3 = 0.1$	75.1	3.8	39.5	0.699
$w_1 = 0.8$, $w_2 = 0.1$, $w_3 = 0.1$	82.2	11.2	42.2	0.784

When cost is heavily prioritized ($w_3 = 0.8$), the deployment cost is reduced to 33.1%, but coverage drops to 75.8% and interference increases slightly to 6.8%. This configuration yields a fitness value of 0.733, indicating that excessive cost minimization may compromise solution quality. In contrast, strongly emphasizing interference minimization ($w_2 = 0.8$) leads to the lowest interference level (3.8%), but also reduces coverage (75.1%) and increases cost (39.5%), resulting in the lowest fitness value (0.699). This suggests that aggressively minimizing interference alone is not sufficient for achieving an optimal solution. Finally, assigning a dominant weight to coverage ($w_1 = 0.8$) produces the highest coverage (82.2%), but also leads to the highest interference (11.2%) and cost (42.2%). Nevertheless, this configuration achieves the highest fitness value (0.784), indicating that under this scenario, improving coverage has a stronger positive impact on the overall objective despite the associated penalties.

The sensitivity analysis results of the fitness function weights in this section demonstrate that the KBGWO-RNP model effectively adapts to different optimization priorities. However, extreme weight settings tend to amplify trade-offs among objectives, whereas balanced or moderately coverage-oriented configurations provide more efficient solutions for RNP. It should be emphasized that all results in this section are obtained under Scenario C2, where the minimum coverage constraint (COV_{min}) is set to exceed 75%. Any variation in this constraint would significantly influence the results, potentially leading to more pronounced differences than those reported in Table 11.

5.6 Sensitivity Analysis of Criticality Map

In this subsection, the robustness of the KBGWO-RNP model is evaluated using 10 different randomly generated criticality maps on the hospital plan of Fig. 5. This analysis introduces variability in spatial criticality distributions to simulate asset importance as non-uniform. Each map assigns different criticality levels to grid cells, while preserving the same physical layout (walls, corridors, and accessible areas). The model is executed independently on each map under the three scenarios C1, C2, and C3.

Table 12 summarizes the overall fitness function values obtained across all maps. The results demonstrate that KBGWO-RNP maintains consistent performance across varying criticality patterns. Although slight fluctuations are observed, the variance remains limited, indicating that the model effectively adapts antenna placement strategies based on spatial importance distributions.

Table 12: Obtained fitness function value for different criticality maps.

Criticality Map #	Scenario C1	Scenario C2	Scenario C3
1	0.824	0.749	0.631
2	0.818	0.742	0.625
3	0.829	0.753	0.634
4	0.821	0.747	0.628
5	0.843	0.766	0.647
6	0.817	0.739	0.623
7	0.806	0.741	0.612
8	0.820	0.746	0.627
9	0.811	0.734	0.618
10	0.822	0.748	0.629

5.7 Statistical Analysis

To evaluate the robustness and statistical reliability of the KBGWO-RNP model, a comprehensive statistical analysis is performed using the results obtained from the 10 different criticality maps reported in Table 12. In addition to descriptive statistics, dispersion measures and inferential tests are employed to assess the consistency and significance of the model's performance. It should be noted that the statistical analysis evaluates variability across different criticality-map realizations (reported in Section 5.6), rather than repeated stochastic executions over a fixed map configuration.

Table 13 presents the mean, standard deviation, coefficient of variation, and 95% confidence interval of the fitness values for each scenario. The results show that KBGWO-RNP maintains a high level of stability across all scenarios. The standard deviation values are low (approximately 0.010), and the coefficient of variation remains close to 1%–1.5%, indicating limited sensitivity to variations in the criticality maps. Scenario C1 exhibits slightly higher variability due to the more flexible solution space under relaxed constraints, whereas Scenarios C2 and C3 show comparable and stable behavior despite stricter requirements. The relatively narrow confidence intervals confirm the statistical reliability of the obtained mean values.

Table 13: Statistical analysis of KBGWO-RNP over 10 criticality maps.

Metric	Scenario C1	Scenario C2	Scenario C3
Mean Fitness	0.821	0.747	0.627
Std. Deviation	0.0104	0.0092	0.0096
Coefficient of Variation (%)	1.27%	1.23%	1.53%
95% Confidence Interval	[0.814, 0.828]	[0.741, 0.753]	[0.621, 0.633]
Friedman Test (p-Value)	$p < 0.05$	$p < 0.05$	$p < 0.05$
Wilcoxon Pairwise Tests	$p < 0.05$ for all pairs	$p < 0.05$ for all pairs	$p < 0.05$ for all pairs

To examine the statistical significance of performance differences, a non-parametric Friedman test is conducted across the three scenarios using the results from Table 12. The test indicates statistically significant differences among the scenarios ($p < 0.05$), which is consistent with the increasing coverage constraints. Furthermore, post-hoc Wilcoxon signed-rank tests confirm that all pairwise differences between scenarios are statistically significant ($p < 0.05$). Overall, these results demonstrate that the KBGWO-RNP model provides not only strong optimization performance but also consistent and statistically reliable results under varying spatial conditions.

5.8 Ablation Study

To assess the contribution of each component in the proposed KBGWO-RNP framework, an ablation study is conducted by comparing three configurations:

- **KBH-only** (heuristic-based placement without metaheuristic search): For the KBH-only configuration, an initial solution is randomly generated. Then, the KBH-based improvement procedure (as seen in Fig. 4) is applied iteratively to all deployed antennas i across all grid locations g.
- **GWO-only** (metaheuristic-based placement without knowledge-based guidance): For the GWO-only configuration, the KBH model is removed from the KBGWO-RNP flowchart of Fig. 2. In this setting, only the standard GWO operators are applied to solve the RNP problem.
- **KBGWO-RNP** (the full version of the proposed model as seen in Fig. 2).

The ablation study results over the 10 criticality maps, are presented in Table 14. The KBH-only configuration, which serves as the baseline heuristic method, achieves the lowest fitness values across all scenarios. Its main advantage lies in computational efficiency, as reflected in its very low running times (0.12–0.15 s). However, this efficiency comes at the cost of limited exploration capability and reduced robustness. This behavior is reflected in the relatively high standard deviation values (0.0283, 0.0270, and 0.0266), which indicate strong sensitivity to map variations and inconsistent convergence behavior across different deployments. In contrast, the GWO-only configuration improves fitness performance across all scenarios, achieving values of 0.798, 0.720, and 0.595. This improvement is attributed to the stronger global search capability of the GWO, which enables broader exploration of the solution space than a heuristic search method. Moreover, the standard deviation values decrease significantly to 0.0092, 0.0096, and 0.0087, showing that the metaheuristic search provides more stable solutions and better adaptability to varying criticality maps. However, this comes with a significant computational cost, as reflected in the substantially higher running times (74–83 s).

Table 14: Ablation study results (average over 10 maps).

Method	Fitness Function Value (Mean ± Std)		
	Scenario C1	**Scenario C2**	**Scenario C3**
KBH	0.746 ± 0.0283	0.642 ± 0.0270	0.511 ± 0.0266
GWO	0.798 ± 0.0092	0.720 ± 0.0096	0.595 ± 0.0087
KBGWO-RNP	0.821 ± 0.0034	0.747 ± 0.0030	0.627 ± 0.0031
Method	**Running Time (Seconds)**		
	Scenario C1	**Scenario C2**	**Scenario C3**
KBH	0.12	0.13	0.15
GWO	74	77	83
KBGWO-RNP	78	82	90

The proposed KBGWO-RNP hybrid model consistently achieves the best fitness performance across all scenarios, with values of 0.821, 0.747, and 0.627. This improvement comes with a slight increase in computational cost compared to GWO-only, with running times of 78–90 s. More importantly, the hybrid model achieves the lowest standard deviation values (0.0031–0.0034), indicating highly stable and consistent performance across all tested maps. The very small variance demonstrates that the integration of knowledge-based refinement with global optimization not only improves solution quality but also enhances convergence reliability and robustness against environmental variations.

These results highlight a clear trade-off between computational efficiency and solution quality across the three methods. KBH provides extremely fast execution but suffers from weak exploration capability and high variability. GWO significantly improves solution quality and stability but at a high computational cost. In contrast, the proposed hybrid KBGWO-RNP framework achieves the best balance between these two extremes by combining strong global exploration with informed local refinement, resulting in superior fitness performance, lower variability, and more reliable convergence behavior.

6 Conclusion

In this work, we presented a hybrid heuristic-metaheuristic framework, named KBGWO-RNP, for RFID network design in hospital environments. The proposed model was motivated by the need to overcome both modeling simplifications and algorithmic shortcomings observed in existing RNP methods. KBGWO-RNP combines domain-specific heuristic knowledge with the global search capability of GWO to guide antenna placement decisions during the metaheuristic-based search process. The model supports heterogeneous directional antennas, allowing to flexibly select antenna gain, read range, beam width, and cost based on spatial and operational requirements. Experimental evaluations conducted on a hospital layout under multiple coverage scenarios show that KBGWO-RNP adapts to varying operational constraints and clearly captures the trade-off between coverage, interference, and cost. The results demonstrate that KBGWO-RNP achieves higher coverage with lower interference and reduced deployment cost compared to existing approaches. Unlike conventional metaheuristics that mainly depend on random population updates, the proposed model embeds domain-specific knowledge into the search process, enabling solutions to be refined progressively and efficiently, while reducing the need for expensive global exploration.

Despite the advantages of the proposed model, several extensions can further enhance its applicability. Although the proposed method demonstrates acceptable computational performance for moderately large environments, further optimization and parallelization strategies may be required to efficiently handle very large-scale hospital layouts with higher spatial resolution and dense deployment requirements. The current knowledge-based heuristic model relies on a limited set of spatial and structural indicators, and thus, incorporating additional factors such as path-loss variability, signal attenuation due to medical equipment, dynamic obstacles (e.g., staff and patients), and energy consumption of readers could improve realism in complex hospital settings. The current model assumes a static environment and does not explicitly account for dynamic factors such as time-varying asset movement, environmental changes, or adaptive reconfiguration of the network. Extending the proposed framework to dynamic and real-time RNP, potentially through online optimization or reinforcement learning approaches, represents an important direction for future research. Additionally, the proposed framework should be viewed as an optimization-based planning methodology under simplified indoor propagation assumptions, rather than a full physical-layer RF deployment simulator. Therefore, future work may incorporate more advanced RF effects such as stochastic attenuation, multipath fading, metallic scattering, and device-level channel behavior. Future work will extend the proposed framework by incorporating advanced multi-objective optimization techniques such as NSGA-III and MOEA/D, as well as exploring data-driven and deep learning-based approaches. Finally, integrating security- and privacy-aware constraints, which are critical in healthcare RFID deployments, could further broaden the framework's relevance and practical impact.

Acknowledgement: Not applicable.

Funding Statement: The authors received no specific funding for this study.

Author Contributions: The authors confirm contribution to the paper as follows: conceptualization, Mohamad Khairi Ishak, Samir Ait Lhadj Lamin and Mohammad Shokouhifar; methodology, Mohamad Khairi Ishak, Samir Ait Lhadj Lamin, Mohammad Shokouhifar and Kamal M. Othman; software, Mohamad Khairi Ishak, Samir Ait Lhadj Lamin and Mohammad Shokouhifar; validation, Samir Ait Lhadj Lamin and Mohammad Shokouhifar; formal analysis, Aseel Smerat and Kamal M. Othman; investigation, Samir Ait Lhadj Lamin, Aseel Smerat, Abdulfattah Noorwali and Esam Y.O. Zafar; data curation, Samir Ait Lhadj Lamin and Mohammad Shokouhifar; writing—original draft preparation, Mohamad Khairi Ishak, Samir Ait Lhadj Lamin, Mohammad Shokouhifar and Aseel Smerat; writing—review and editing, Mohammad Shokouhifar, Kamal M. Othman, Abdulfattah Noorwali and Esam Y.O. Zafar; visualization, Samir Ait Lhadj Lamin, Abdulfattah Noorwali and Esam Y.O. Zafar; supervision, Mohammad Shokouhifar; project administration, Mohammad Shokouhifar and Kamal M. Othman. All authors reviewed and approved the final version of the manuscript.

Availability of Data and Materials: Data available on request from the authors.

Ethics Approval: Not applicable.

Conflicts of Interest: The authors declare no conflicts of interest.

References

1. Stoica M, Nitu AI. Tracking patient movements using an IoT and RFID system—A case study in a Romanian clinic. Logistics. 2025;9(1):34. doi:10.3390/logistics9010034.
2. Bui CD, Narbudowicz A. Dual-polarized chipless RFID tag with simultaneous identification and sensing. IEEE Trans Antennas Propagat. 2025;73(8):5708–15. doi:10.1109/tap.2025.3566221.
3. Ait Lhadj Lamin S, Raghib A, Abou El Majd B. Robust multi-objective optimization for solving the RFID network planning problem. Math Model Comput. 2021;8(4):616–26. doi:10.23939/mmc2021.04.616.
4. Van Hoa L, Van Tung N, Nhat VVM. An approach to Hopfield network-based energy-efficient RFID network planning. Cybern Inf Technol. 2024;24(2):50–66. doi:10.2478/cait-2024-0015.

5. Guo G, Yang X, Liang Z, Xi Z, Zhan X, Li P. Adaptive RFID data scheduling using proximal policy optimization for reducing data processing latency. IEEE Access. 2025;13(1):68340–50. doi:10.1109/ACCESS.2025.3562127.
6. Shokouhifar M, Fanian F, Kuchaki Rafsanjani M, Hosseinzadeh M, Mirjalili S. AI-driven cluster-based routing protocols in WSNs: a survey of fuzzy heuristics, metaheuristics, and machine learning models. Comput Sci Rev. 2024;54(4):100684. doi:10.1016/j.cosrev.2024.100684.
7. Camacho-Cogollo JE, Bonet I, Iadanza E. RFID technology in health care. In: Clinical engineering handbook. Cambridge, MA, USA: Academic Press; 2020. p. 33–41.
8. Seol S, Lee EK, Kim W. Indoor mobile object tracking using RFID. Future Gener Comput Syst. 2017;76(1):443–51. doi:10.1016/j.future.2016.08.005.
9. Pantoja E, Gao Y, Yin J, Stan MR. Virtualized computational RFID (VCRFID) solution for industry 4.0 applications. Electronics. 2025;14(12):2397. doi:10.3390/electronics14122397.
10. Lyu W, Barati M, Mirzavand R. A streamlined two-antenna architecture for passive RFID phase localization via accelerometer-based yaw disambiguation. IEEE Sens J. 2026;26(7):11176–87. doi:10.1109/JSEN.2026.3661293.
11. Veloo SG, Tiang JJ, Muhammad S, Wong SK. A hybrid solar-RF energy harvesting system based on an EM4325-embedded RFID tag. Electronics. 2023;12(19):4045. doi:10.3390/electronics12194045.
12. Solar H, Beriain A, Berenguer R, Sosa J, Montiel-Nelson JA. Semi-passive UHF RFID sensor tags: a comprehensive review. IEEE Access. 2023;11:135583–99. doi:10.1109/ACCESS.2023.3336761.
13. Szabó R, Nikolić L, Sarang S, Sharif A, Drieberg M, Stojanović GM. Textile-based green energy assisted UHF RFID tag with enhanced read range. In: Proceedings of the 2026 IEEE International Conference on Consumer Electronics (ICCE); 2026 Feb 3–5; Dubai, United Arab Emirates. p. 1–5.
14. Gupta N, Iyer S. RFIDPlanner—A coverage planning tool for RFID networks. Lect Notes Comput Sci. 2005;3823:1047–57.
15. Mysore N, Nenavat P, Unnithan RS, Mulukutla R, Rao S. An efficient algorithm for RFID reader positioning for coverage of irregularly-shaped areas. In: Proceedings of the 2009 IEEE International Conference on Automation Science and Engineering; 2009 Aug 22–25; Bangalore, India. p. 233–40.
16. Liu X, Xiao B, Zhu F, Zhang S. Let's work together: Fast tag identification by interference elimination for multiple RFID readers. In: Proceedings of the 2016 IEEE 24th International Conference on Network Protocols (ICNP); 2016 Nov 8–11; Singapore. p. 1–10.
17. Qu X, Simpson LT, Stanfield P. A model for quantifying the value of RFID-enabled equipment tracking in hospitals. Adv Eng Inform. 2011;25(1):23–31. doi:10.1016/j.aei.2010.05.005.
18. Tsai MH, Pan CS, Wang CW, Chen JM, Kuo CB. RFID medical equipment tracking system based on a location-based service technique. J Med Biol Eng. 2019;39(1):163–9. doi:10.1007/s40846-018-0446-2.
19. Nhat VVM. An artificial neural network-based RFID network planning method for asset monitoring in healthcare. Int J Fuzzy Log Intell Syst. 2024;24(3):181–93. doi:10.5391/ijfis.2024.24.3.181.
20. Wang Y, Kamaludin H, Mohammed Alduais NA, Zuraidin Mohd Safar N, Hao Z. RFID network planning of smart factory based on swarm intelligent optimization algorithm: A review. IEEE Access. 2024;12(8):64980–96. doi:10.1109/access.2024.3397402.
21. Dimitriou AG, Siachalou S, Bletsas A, Sahalos J. Introduction of dynamic virtual force vector in particle swarm optimization for automated deployment of RFID networks. In: Proceedings of the 2019 13th European Conference on Antennas and Propagation (EuCAP); 2019 Mar 31–Apr 5; Krakow, Poland. p. 1–5.
22. Shi W, Guo Y, Yan S, Yu Y, Luo P, Li J. Optimizing directional reader antennas deployment in UHF RFID localization system by using a MPCSO algorithm. IEEE Sens J. 2018;18(12):5035–48. doi:10.1109/JSEN.2018.2832216.
23. Jaballah A, Meddeb A. A new variant of cuckoo search algorithm with self adaptive parameters to solve complex RFID network planning problem. Wirel Netw. 2019;25(4):1585–604. doi:10.1007/s11276-017-1616-9.
24. Zhang Z, Ren J, Dai Z, Zhang B, Wu L, Wu Z. Research on RFID network planning based on directional and omnidirectional antenna readers. In: Advances in natural computation, fuzzy systems and knowledge discovery. Cham, Switzerland: Springer International Publishing; 2021. p. 1192–202.
25. Zhu W, Li M. RFID reader planning for the surveillance of predictable mobile objects. Procedia Comput Sci. 2018;129(11):475–81. doi:10.1016/j.procs.2018.03.027.

26. Xu B, Li J, Yang Y, Postolache O, Wu H. Robust modeling and planning of radio-frequency identification network in logistics under uncertainties. Int J Distrib Sens Netw. 2018;14(4):1550147718769781. doi:10.1177/1550147718769781.
27. Yuan C, Chen H, Shen J, Lin N, Su W, Liu F, et al. Indicator-based multi-objective adaptive bacterial foraging algorithm for RFID network planning. Clust Comput. 2019;22(5):12649–57. doi:10.1007/s10586-018-1715-0.
28. Shokouhifar M. Swarm intelligence RFID network planning using multi-antenna readers for asset tracking in hospital environments. Comput Netw. 2021;198(1):108427. doi:10.1016/j.comnet.2021.108427.
29. Mohammed SQ, Abdullah MN, Al-Araji AS. Hybrid swarm intelligence algorithm design for optimizing RFID-NP. Wirel Pers Commun. 2023;34(1):1–31. doi:10.1007/s11277-023-10706-8.
30. Knapp H, Romagnoli G. RFID systems optimisation through the use of a new RFID network planning algorithm to support the design of receiving gates. J Intell Manuf. 2023;34(3):1389–407. doi:10.1007/s10845-021-01858-0.
31. Zheng J, Lin Z, Xie X. Improved multi-objective brain storm optimization algorithm for RFID network planning. Wirel Netw. 2024;30(2):1055–68. doi:10.1007/s11276-023-03543-x.
32. Abdulbaqi HA, Abdullah AL-Khalidi FQ. Evaluation software and IT integration for IoT-based healthcare radio frequency identification network planning. Fusion Pract Appl. 2024;15(2):288–97. doi:10.54216/fpa.150224.
33. Maimouni M, Abou El Majd B, Bouya M. Optimising RFID network planning problem using an improved automated approach inspired by artificial neural networks. Inf Sci. 2025;703:121927. doi:10.1016/j.ins.2025.121927.
34. Ma L, Hu K, Zhu Y, Chen H. Cooperative artificial bee colony algorithm for multi-objective RFID network planning. J Netw Comput Appl. 2014;42(3):143–62. doi:10.1016/j.jnca.2014.02.012.
35. Lu S, Yu S. A fuzzy k-coverage approach for RFID network planning using plant growth simulation algorithm. J Netw Comput Appl. 2014;39(7):280–91. doi:10.1016/j.jnca.2013.07.015.
36. Hosseinzadeh M, Elbatal I, Abdelwahab MM, Smerat A, Shokouhifar M, Wagdy Mohamed A. AMORT-FIS: Adaptive metaheuristic-optimized real-time fuzzy inference system for RFID network planning using heterogeneous directional antennas. AEU Int J Electron Commun. 2026;203(1):156061. doi:10.1016/j.aeue.2025.156061.
37. Lamin SAL, Elbatal I, Abdelwahab MM, Othman KM, Ishak MK, Shokouhifar M, et al. Fuzzy knowledge-based ant colony optimization for sequential RFID network design in hospitals using heterogeneous readers and antennas. AEU Int J Electron Commun. 2026;205(2):156152. doi:10.1016/j.aeue.2025.156152.
38. Gharaei N, Alabdali AM. Optimizing smart health monitoring systems: enahancing energy efficiency and reducing latency with multi-level clustering and grey wolf optimizer. Clust Comput. 2024;28(2):87. doi:10.1007/s10586-024-04811-x.
39. Stephan T, Punitha S, Lin CC, Agarwal S. A comprehensive study of grey wolf optimizer variants for optimizing feature selection in high-dimensional data. Appl Artif Intell. 2026;40(1):2601378. doi:10.1080/08839514.2025.2601378.